Toward NZEB in Public Buildings: Integrated Energy Management Systems of Thermal and Power Networks

Ana Beatriz Soares Mendes, Carlos Santos Silva, and Manuel Correia Guedes

Introduction

In recent years, climate change and environmental degradation have grown to be major threats to the well-being of the global population.

The European Commission has required each EU member state to establish a 10-year integrated national energy and climate plan (NECP) for the period of 2021–2030 [1].

Buildings are one of the largest energy consumer sectors in Europe, being responsible for approximately 40% of EU energy consumption and 36% of its greenhouse gas (GHG) emissions [2].

Nearly zero energy buildings (nZEB) have a very high energy performance, which means that they have low energy needs being largely covered by energy from renewable sources, produced onsite or nearby. Therefore, the renovation and rehabilitation of the existing buildings turning them into nZEB are also a priority in the Portuguese NECP, making it possible to achieve other objectives such as a reduction in energy bills and emissions and an improvement in the levels of health and comfort of these buildings [3]. In Portugal, a commerce and services building is considered nZEB when the maximum value of the energy efficiency indicator is equal or smaller than 75% of the reference value and the energy class ratio is not greater than 0.50 [4].

The first step for the conception of nZEB buildings is the integration of bioclimatic/passive design strategies in their architectural project. This step can allow for a reduction in energy needs of up to 60% (thermal and lighting) compared with conventional buildings. Renewable energy systems will provide the remaining

A. B. S. Mendes · C. S. Silva · M. C. Guedes (✉)
Instituto Superior Técnico, Universidade de Lisboa, Lisbon, Portugal
e-mail: manuel.guedes@tecnico.ulisboa.pt

A. Sayigh (ed.), *Towards Net Zero Carbon Emissions in the Building Industry*, Innovative Renewable Energy, https://doi.org/10.1007/978-3-031-15218-4_13

energy needs, being the complement (rather than the remedy) to a good building design. This articulation between bioclimatic design and renewable energy systems should be considered in the first stages of the project – as was the case of the LNEG building.

The local small-scale power supply technologies and storage systems for energy consumption in buildings, such as microgrids, will play a key role in the future power system. They offer environmental benefits, by using locally produced renewable energy; social benefits, due to their reliability, affordability, and resilience; and economic benefits, by increasing self-sufficiency.

The main objective of this work is to develop integrated energy management strategies for thermal and power networks in a building. This work will focus on the study of a microgrid implemented on a pilot bioclimatic office building at *Laboratório Nacional de Energia e Geologia* (LNEG), part of the IMPROVEMENT research project that aims to transform existing public buildings into nZEB, integrating renewable energy microgrids with combined heat, cold, and electricity generation as well as storage systems [5].

Literature Review

Microgrids

According to the US Department of Energy, a microgrid (MG) is a "group of interconnected loads and distributed energy resources (DERs) within clearly defined electrical boundaries that acts as a single controllable entity with respect to the grid" and which has the capability to "connect and disconnect from the grid to enable it to operate in both grid-connected or islanded-mode" [6].

A MG consists of loads, DERs, a control system, and a point of common coupling (PCC). DERs are composed of distributed generation (DG) units, which may include, for example, solar photovoltaic (PV) panels, wind turbines, combined heat and power generators, and energy storage systems (ESS). In grid-connected mode, ESS establishes optimal periods to interchange power with the utility grid in a more convenient way. Thus, ESSs improve the reliability of the system and support the DGs when they cannot supply the full power required by the consumers [7].

Microgrid Energy Management Systems

An energy management system (EMS) is an information and control system that ensures that generation, transmission, and distribution supply energy at a minimum cost [8]. MG involves a software that optimizes the operation of the system by

considering the two MG operation modes (isolated and interconnected) and the minimal required cost of operation [9].

Control Structure

Two approaches to the control structure were identified: centralization and decentralization. In a centralized control system, the data from all components is gathered into a central controller (CC) that performs the required calculations and determines the control actions for all the units at a single point. The CC uses the input data to solve the optimization problem and then transmits the optimal control decisions, through local controllers (LCs), to the correspondent DERs, where they are implemented. In a decentralized (or distributed) control system, there is no CC, and several LCs are set up to measure signals of the different DERs [10].

A compromise between fully centralized and fully decentralized control schemes is achieved by means of a hierarchical control scheme [11] with three control levels: primary, secondary, and tertiary. They differ in (i) their speed of response and the time frame in which they operate as well as (ii) infrastructure requirements [12].

Control Strategies

According to [11], most studies use model predictive control (MPC) strategies and optimal control, followed by multiagent systems (MAS) and rule-based control (RBC).

RBC is a static control strategy that relies on "IF-THEN" commands. It is popular in commercial building automation systems, because it is simple to implement [13]. It does not require any future data profile to make a decision and is thus suitable for real-time applications [14]. Homeostatic control (HC) is a form of RBC that employs an adaptive strategy that balances positive and negative feedback mechanisms, inspired by the biological concept of homeostasis.

Optimal control aims to optimize an objective function, subject to a set of constraints [15]. Such methods are often divided into three categories: classical, metaheuristic, and stochastic. In MG applications, the objective is systematically to minimize the total operational cost but may also have a second objective, e.g., minimizing GHG emissions or occupant thermal discomfort or considering undesirable outcomes by introducing a corresponding penalty. Common decision variables are: the amount of power that is taken from each dispatchable source; requested from the grid at each time; injected into the grid; charged to or discharged from a battery; reactive power support from renewable energy systems and/or batteries; state of charge (SOC) of ESS; controllable loads; and temperature setpoints.

A MAS is a collection of intelligent agents that interact with each other in such a way that the entire system learns and evolves toward a better solution. MGs allow coordination and control in a decentralized way [16].

MPC encompasses a set of control methods that rely on the dynamic model of the studied system [17]. Here, the current state of the system and its model and outside disturbances are inputs of the controller, which in turn outputs the future state of the system. It has the advantage of considering the future state of the system and disturbances, anticipating future events, and acting on that foreknowledge.

State of the Art

The literature covering the situation of EMSs that make use of thermal and power systems simultaneously was found to be sparse. In the following, an overview of the relevant case studies is given.

In [18], HC strategies were used for power management and EMS while considering the thermal behavior of the building. The MG under study contained solar panels, a wind turbine, an inverter, storage based on batteries, an HVAC, and a smart meter to measure the amount of energy that was consumed from the grid or injected to it. It also included multiple temperature and humidity sensors. The control block received as input the power consumption limit from the utility grid, power consumption, SOC of batteries, availability of the utility grid, and temperatures (walls, external and internal). The outputs were on-off for the grid selector, the battery, and the HVAC selector. There were two parts to the control strategy, a reactive part that ensured that the batteries had enough charge to maintain the MG running and a predictive one that used the thermal model of the room to maintain the temperatures within the comfortable interval.

In [19], a grid-connected MG located in a sport center facility was investigated through dynamic simulations, considering thermal and electrical loads. This MG was composed of a solar PV installation, a building energy storage system, and a heat pump. The goal was to balance self-sufficiency with electricity cost. To this end, two RBC strategies were employed, taking into account the impact of an HVAC system and of the heat pump. These strategies involved (1) peak shaving of the MG consumption with off-peak grid power and (2) pricing-based operation of the building energy storage system, according to the main grid electricity price. To benchmark the strategies, the resulting power flows and electricity costs were assessed. This analysis revealed that strategy 2 yielded the best results.

In [20], systems consisting of HVAC, battery energy storage and renewable generation in buildings were approached through an optimal control framework. In this case, the goal was to reduce peak load demand and electricity costs while maintaining thermal comfort levels within an acceptable range. The control strategy took into account the thermal dynamics of the building, battery SOC, renewable generation status, and actual operational data and constraints. For the thermal dynamics, a simple model was developed and trained with actual thermal and electrical data. The controller was tested using data from a real building. Preliminary results suggested that it yields a significant reduction in peak electrical power demand.

In [21], an experimental room was considered. It featured temperature, relative humidity, and lighting sensors, as well as an HVAC unit and an electricity microgeneration system with PV panels and an energy storage system. Here, the main objective was to ensure users' comfort and minimize cost, considering electricity

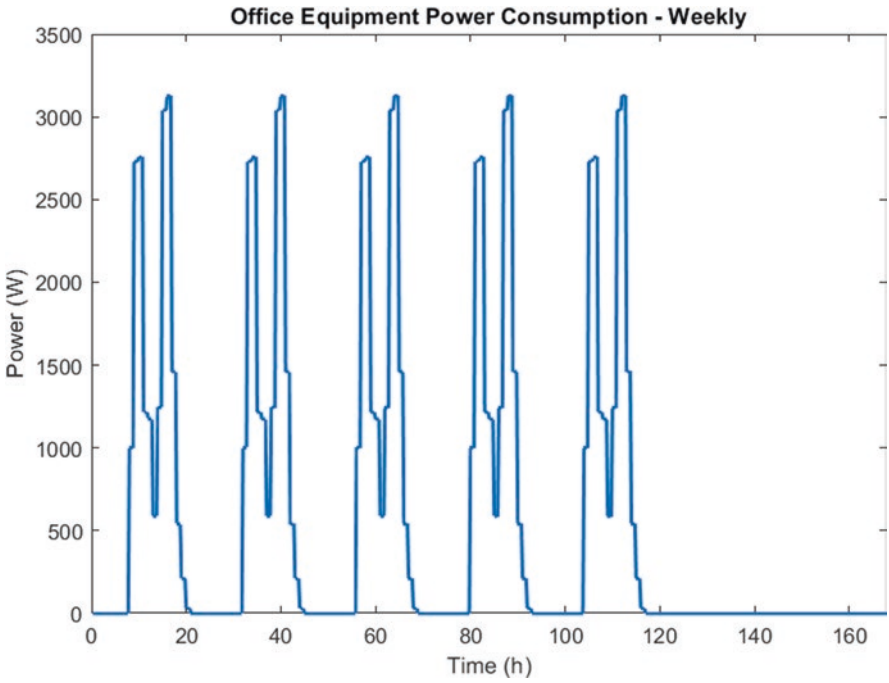

Fig. 1 Office equipment power consumption for a week

price and available energy from renewable sources. To this end, three algorithms were developed: (i) dynamic programming with simplified thermal model, (ii) genetic algorithm with simplified thermal model, and (iii) genetic algorithm with EnergyPlus. They were tested and validated in real conditions and benchmarked against each other. This study found that (iii) generally achieved higher convergence to the optimal value, with more energy being used from the PV system to operate the HVAC. It was noted that the simplified thermal model is less accurate in simulating the indoor temperature (Figs. 1 and 2).

Bioclimatic Building Design

Research on Bioclimatic, or Passive, building design began essentially in the 1970s, during the first oil crisis, and then expanded in the 1990s, with the global warming awareness. The objective of passive design is to reduce the weight of (fossil fuel) energy-consuming mechanical systems in the building, such as HVAC and artificial lighting, through natural means – by taking advantage of the sun's energy for heating and lighting, the local winds for natural ventilation, etc. Today, there are numerous publications on bioclimatic design strategies concerning a variety of climates [22]. These strategies involve design considerations such as solar orientation,

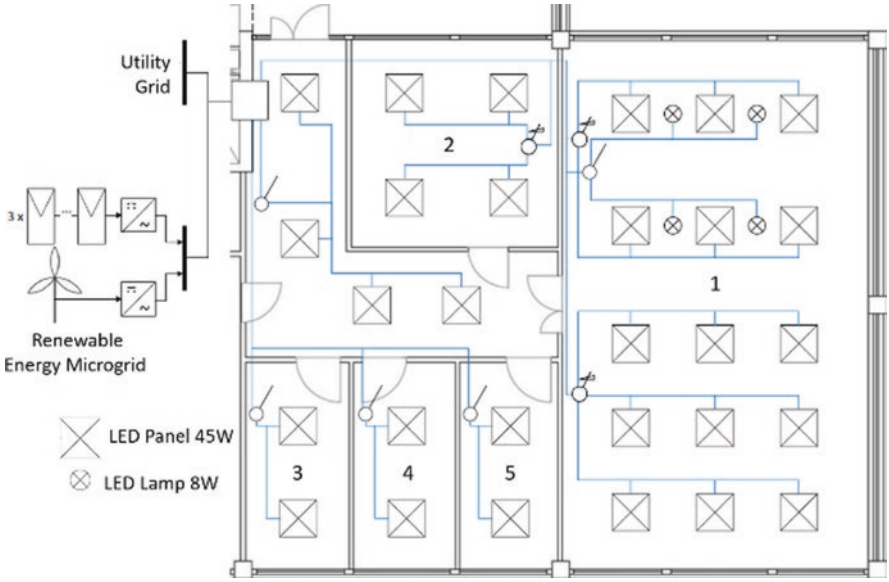

Fig. 2 Building's lighting single-line diagram

building form, shading, insulation, adequate glazing ratio in the facades, thermal inertia, and opening design for ventilation and natural lighting. The LNEG Building followed bioclimatic strategies since the first stages of its design. It is an atrium building (for natural lighting and ventilation), with adequate glazing ratio on the different facades, adequate insulation, and thermal inertia, and uses special passive systems for heating and cooling, such as buried pipes. PVs are embedded in the main (South) façade, doubling as Trombe walls for heating in winter. This bioclimatic approach accounted for a reduction of over 50% of its energy needs (thermal and lighting) from the onset, compared with a conventional office building. It is a fully passive, naturally ventilated building, with no (need for) air-conditioning.

Case Study

The work developed in this study is integrated in the IMPROVEMENT project that has the main goal of converting existing public buildings, which have high energy consumption of electricity, heating, and air conditioning, into nZEB. With this goal in mind, MG pilot plants in LNEG, in Portugal – which, as previously referred, has a bioclimatic building design conception which significantly reduces its energy needs from the onset, i.e., this paper focuses on its complementary renewable energy system design.

The building, represented in Fig. 2, is composed of five rooms and an unconditioned area. Room 1 is a multiuse room, can accommodate 8 people, and has 15

Table 1 Equipment power consumption

Equipment		Power consumption (W)
Desktop		150
Laptop		100
Projector		365
Coffee machine		1560
Printer	Printing/copying	750
	Stand-by	30

45W LED panels and 4 8W LED lamps. Room 2 is a meeting room with a capacity for five people and has four LED panels. Rooms 3, 4, and 5 are individual offices with two LED panels each. The unconditioned space is a small corridor with four LED panels.

The consumption was estimated considering the purpose of each room. It was assumed that the building has one printer and one coffee machine in the corridor. Room 1 has one projector and one desktop. The individual offices have one desktop each and Room 2 two desktops. During the working hours, a variable number of laptops were assumed to be used in the meeting room. The power consumption of each equipment is shown in Table 1. In Fig. 1, the weekly equipment power consumption is displayed considering that the week starts on Monday.

The LNEG MG can be divided into two separate systems: a thermal system and an electrical system. The thermal system is composed of two solar collectors that are 2 m^2 each and have two tanks, one air/water heat pump, a storage tank, and fan coils. The electrical system is made up of five subsystems: four energy generation systems that consist of two PV systems, one with 4050 W and the other with a 560 W rated power; a photovoltaic-thermal (PVT) system with an electricity rated power of 690 W and a 2500 W rated wind power system; and an energy storage system, composed of a 48 V lithium-ion battery with 660-Ah energy capacity and a depth of discharge (DOD) of 85%. The battery has a maximum charging and discharging power of 4200 W.

Thermal and Power Microgrid Integration

Model Integration

As the systems were model in Simulink, the integration itself is done using the same software. Henceforth, the time unit associated with the simulations will be 1 h.

The main difference in the two models was in the solvers. For the electrical model, a fixed time-step (Ts) solver (with Ts necessarily between 1e−5 and 5e−5) with discrete states was used, whereas the thermal model relied on the variable Ts solver ode23s. It was found that the solver ode23t, with a maximum time step of

5e−5, could accommodate the requirements of both models, allowing them to run simultaneously.

Both systems receive weather files as input. They both rely on irradiance and temperature data, and additionally, the electrical model requires wind velocity data. The weather data used was obtained using Meteonorm, with Lisbon as the chosen location and the irradiation values referent to a surface with a tilt angle of 30°.

The second step of the integration was to introduce the thermal model as a subsystem of the electrical model in Simulink. To ensure that the systems were working as intended, a simulation in these conditions was run. It yielded the same results as the separated models, thus confirming the correctness of the implementation so far.

Afterwards, the electrical power of the heat pump was set as a load in the electrical system, together with the office equipment consumption loads.

The thermal model developed in [23] features an on-off control for the heat pump, where the difference between the reference temperature of the storage tank and the observed temperature was used as the control variable. The pump switches on when the temperature of the storage tank is 5 °C lower than the reference temperature, taken to be 50 °C. The pump only switches on if the hot water tank has the capacity to heat the storage tank. To prevent frequent switching of the pump, a minimum operation time is set. This value is equal to 0.1 h (6 min). In the summer, the chosen reference temperature for the heat pump is 10 °C, and a new condition is set to prevent too low temperatures in the hot water tank. The heat pump is always switched off when the tank reaches 7 °C.

The electrical model developed in [24] has a battery charging/discharging control unit responsible for charging the battery when there is simultaneously a surplus in energy generation and the battery SOC is lower than 100% and limited by the charging rate. When the demand surpasses the energy production, this control unit is responsible for discharging the battery until a SOC of 15% is reached, respecting the DOD of 85%. From that point on, if the demand is still higher than the production, the control unit stops discharging the battery to respect the DOD. It is also important to note that when there is a surplus in energy generation and the battery SOC is equal to 100%, the left-over energy is injected into the grid. Similarly, when the demand surpasses the production and the battery SOC equals 15%, the required energy is extracted from the grid. The new model also receives as input the energy tariff. The values were obtained by consulting the website of a Portuguese retailer [25] and correspond to an energy supply tariff scheme with four different periods: super empty, normal empty, floods, and peak. The schedule was consulted in the Entidade Reguladora dos Serviços Energéticos website [26]. The daily term of the price corresponds to 0.7476 €/day, and the power term is divided in two parcels, the peak time power, 0.4874 €/kW.day, and the contracted power, 0.0256 €/kWh.day (Fig. 3). The prices corresponding to each period and the schedule are presented in Table 2.

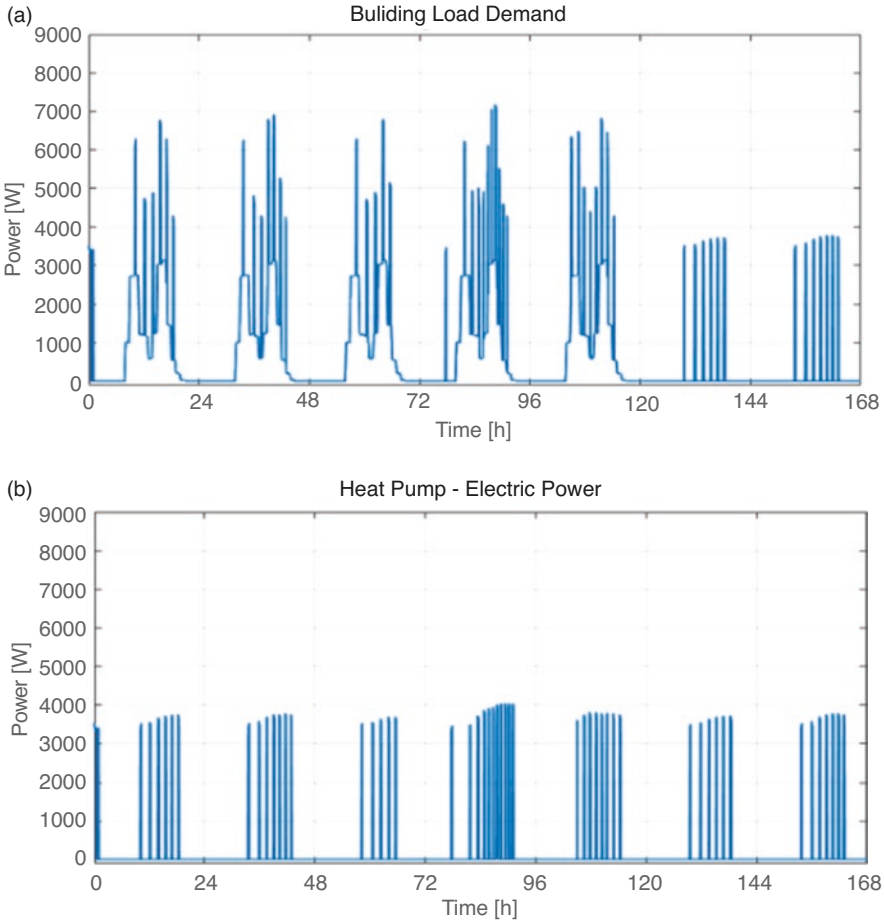

Fig. 3 Building load demand for a week in July: (**a**) total, (**b**) contribution from heat pump

Table 2 Energy prices and schedule of each tariff period

Time Periods Prices (€/kWh)			
Peak	Floods	Normal Empty	Super Empty
	08:00 – 10:30	00:00 – 02:00	
10: 30 – 13:00	13:00 – 19:30	06:00 – 08:00	02:00 – 06:00
19:30 – 21:00	21:00 – 22:00	22:00 – 24:00	
0.2162	0.1329	0.0918	0.0818

Results

Summer

The weather data used in this simulation is referent to a week in the middle of of the week, due to the cooling needs of the space. The heat pump totals a weekly consumption of 40.72 kWh. The generation (Fig. 4) encompasses both the energy-generated values of power by the PV and the wind power systems.

The total energy consumption during the week, 136.3 kWh, represents only 57% of the total energy generated by the MG, 238.8 kWh. Nonetheless, due to the maximum discharging power limit of the battery (4.2 kW), there is the need to extract power from the utility grid. These explain the peaks observed in Fig. 5 that are characterized by a maximum power of 1.87 kW. The total energy consumption from the grid is 1.35 kWh, making up 0.99% of total energy consumption. The energy bill at the end of the week amounts to 5.76€.

Winter

The weather data used in this simulation is referent to the first week of January. As illustrated in Fig. 6, the heat pump behaves quite differently in this season. Instead of switching on and off several times during the day, it does so only four times during the whole week to heat the space. When it does switch on, it reaches a higher maximum power. The weekly consumption of the heat pump is 34.93 kWh. The total energy consumption of the building during the week is130.5 kWh. Henceforth, mentions of power generation for the winter will always refer to Fig. 7. The energy

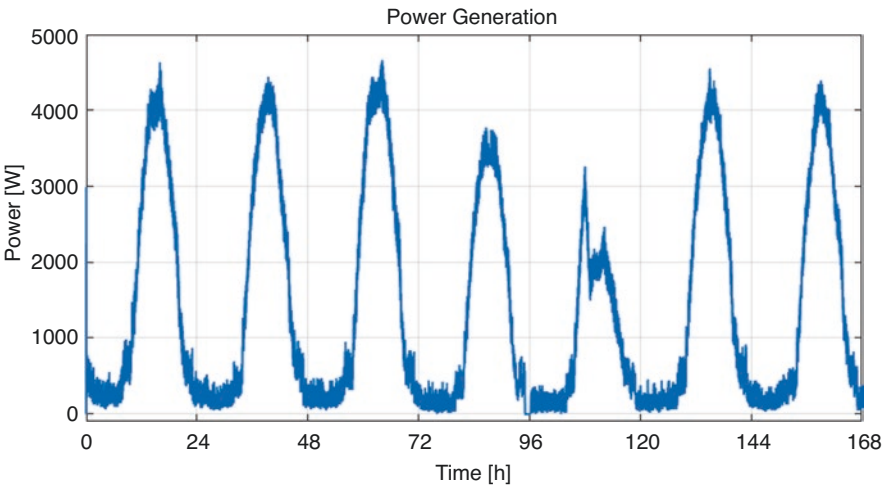

Fig. 4 Power generated by the photovoltaic and wind power systems in a week in July

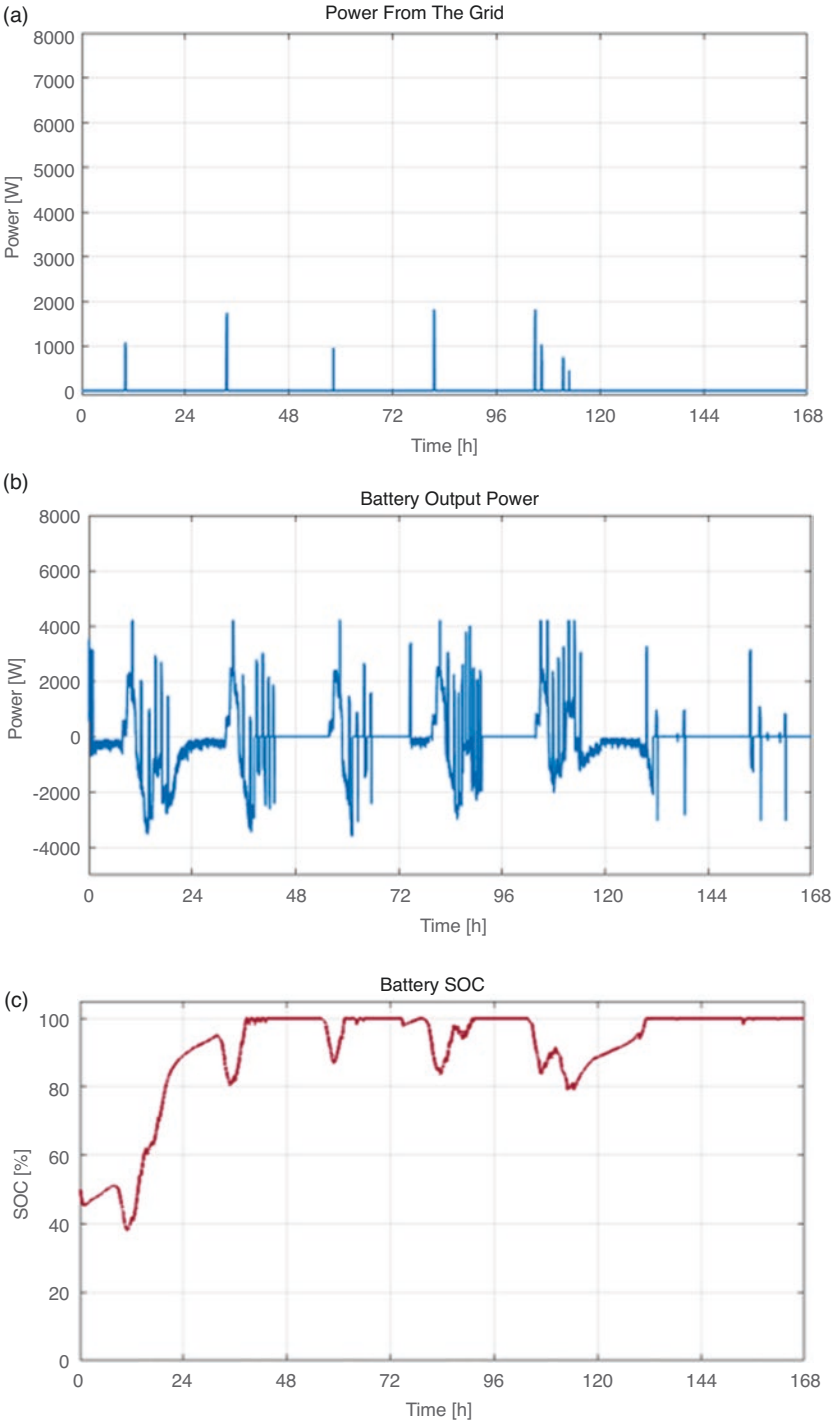

Fig. 5 Microgrid power output for a week in July, (**a**) power extracted from the utility grid, (**b**) battery output power, (**c**) battery SOC

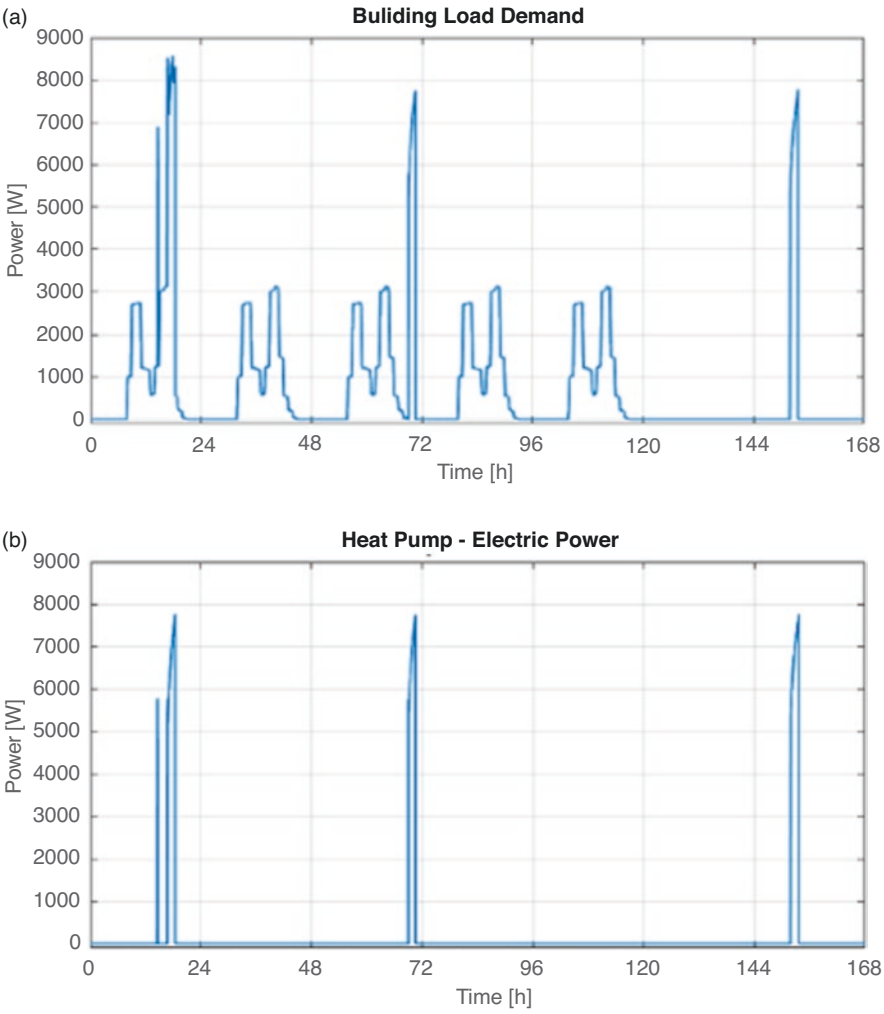

Fig. 6 Building load demand for a week in January: (**a**) total, (**b**) contribution from heat pump

generated by the MG during the entire week is 101.9 kWh, indicating a reduction of 57.3% in relation to the summer values.

From Fig. 8, one notes that the battery SOC is close to its minimum value of 15% for a significant part of the week. The energy extracted from the grid is 45.98 kWh, making up only 35.2% of the total energy consumption. The energy bill increases in relation to the summer to 13,60€.

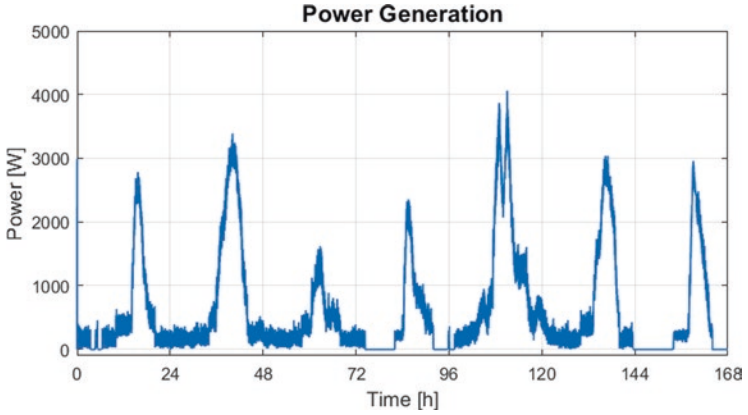

Fig. 7 Power generated by the photovoltaic and wind power systems in a week in January

Modifications to the Case Study

To test some energy management strategies in a case where there is more stress in the battery, i.e., the energy storage is smaller and there are more loads, some modifications to the initial study case were made.

The energy capacity of the battery was reduced from 31,680 Wh (660 Ah, 48 V) to 18,000 Wh (375 Ah, 48 V).

The pilot plant building is part of a main building. It was added to 30% of this building consumption to the pilot plant office equipment power consumption.

Summer

The power consumption curve for the modified study case during the summer week is presented in Fig. 9.

The power consumption from the grid, battery output power, and battery SOC curves are presented in Fig. 10.

During this week, the total energy consumption of the building is 312 kWh, which is 30.65% greater than the energy generation (238.8 kWh). The energy extracted from the utility grid is 97.91 kWh, which is 31.38% of the building load demand. The battery SOC is below 40% for the whole work week. The energy bill at the end of the week is 20.55€.

Winter

Fig. 11 presents the building power consumption curve.

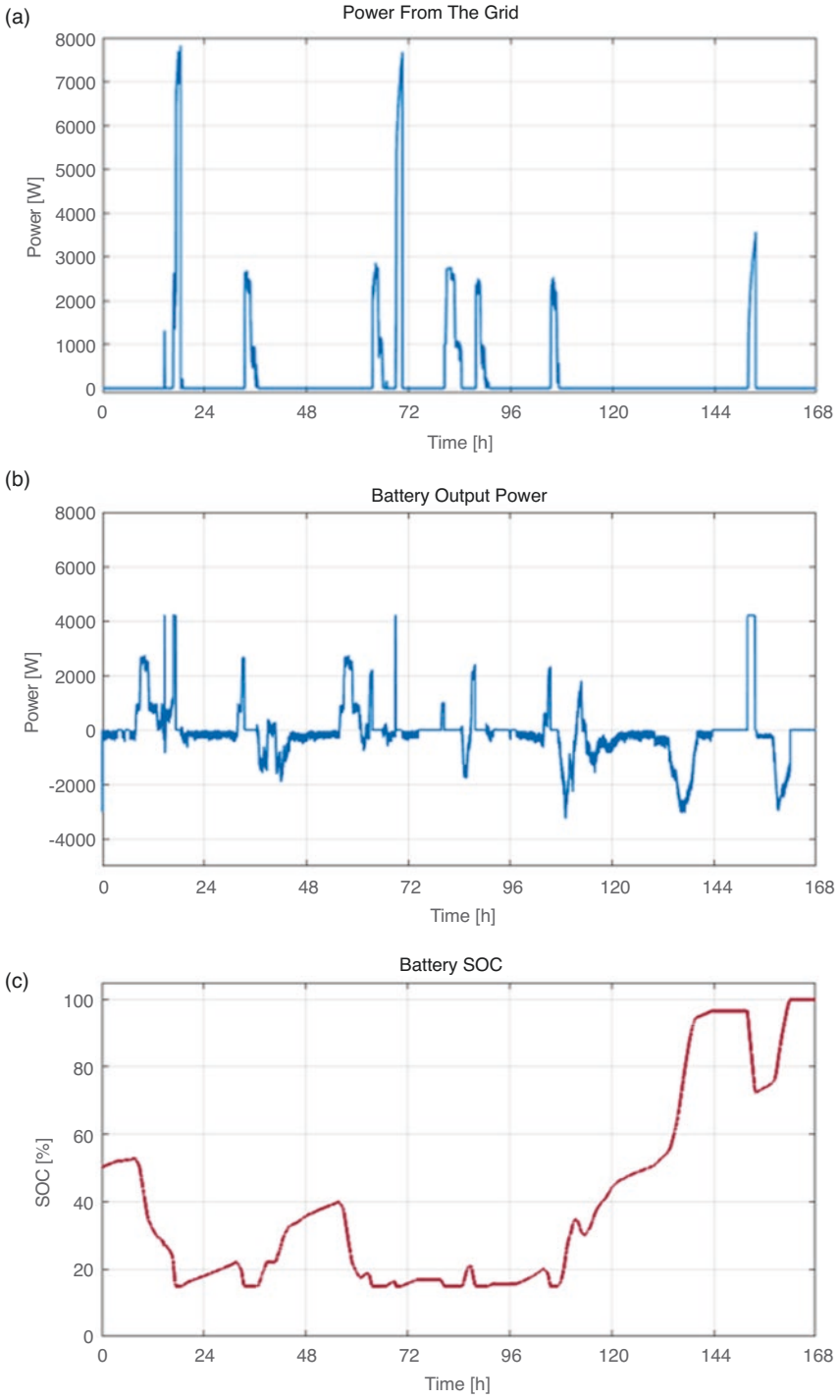

Fig. 8 Microgrid power outputs for a week in January: (**a**) power extracted from the utility grid, (**b**) battery output power, (**c**) battery SOC

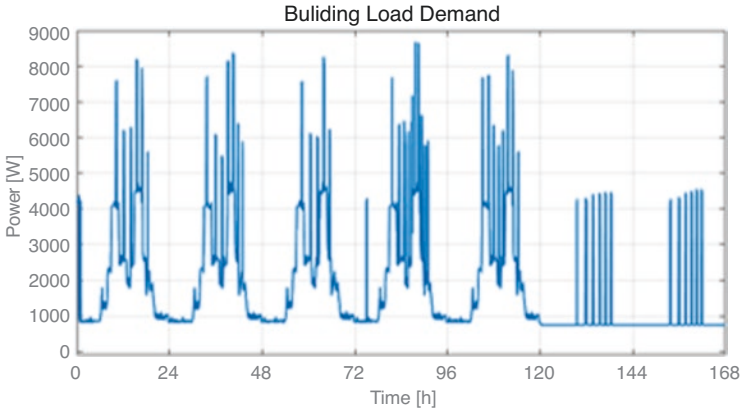

Fig. 9 Microgrid building load demand for the modified case in summer

The power consumption from the grid, battery output power, and battery SOC during the first week of January are presented in Fig. 12.

The total energy consumption during this week is 306.2 kWh, which is three times greater than the energy generated by the MG, and the energy extracted from the grid is 199.8 kWh, which is 65.28% of the energy consumption.

From the battery output power and battery SOC graphs, it can be concluded that the battery is, for most of the time, at its minimum SOC. The energy bill for this case is 38.19€.

Energy Management System

Two different control strategies following a rule-based control approach were developed. The base case, from section "Thermal and Power Microgrid Integration", from now on will be referred to as case without EMS, because the EMS was not integrated.

Control Strategy 1

The first management algorithm developed was based on the real-time electricity pricing signal and the SOC of the battery. It was focused on the economic dispatching of the storage system, charging the battery with power from grid when the energy prices are lower, storing this energy so it can be used when the price value increases.

Thus, when the SOC is between 30% and 90%, if the price of energy is equal or smaller than the quartile of energy prices during that day, the battery charges with

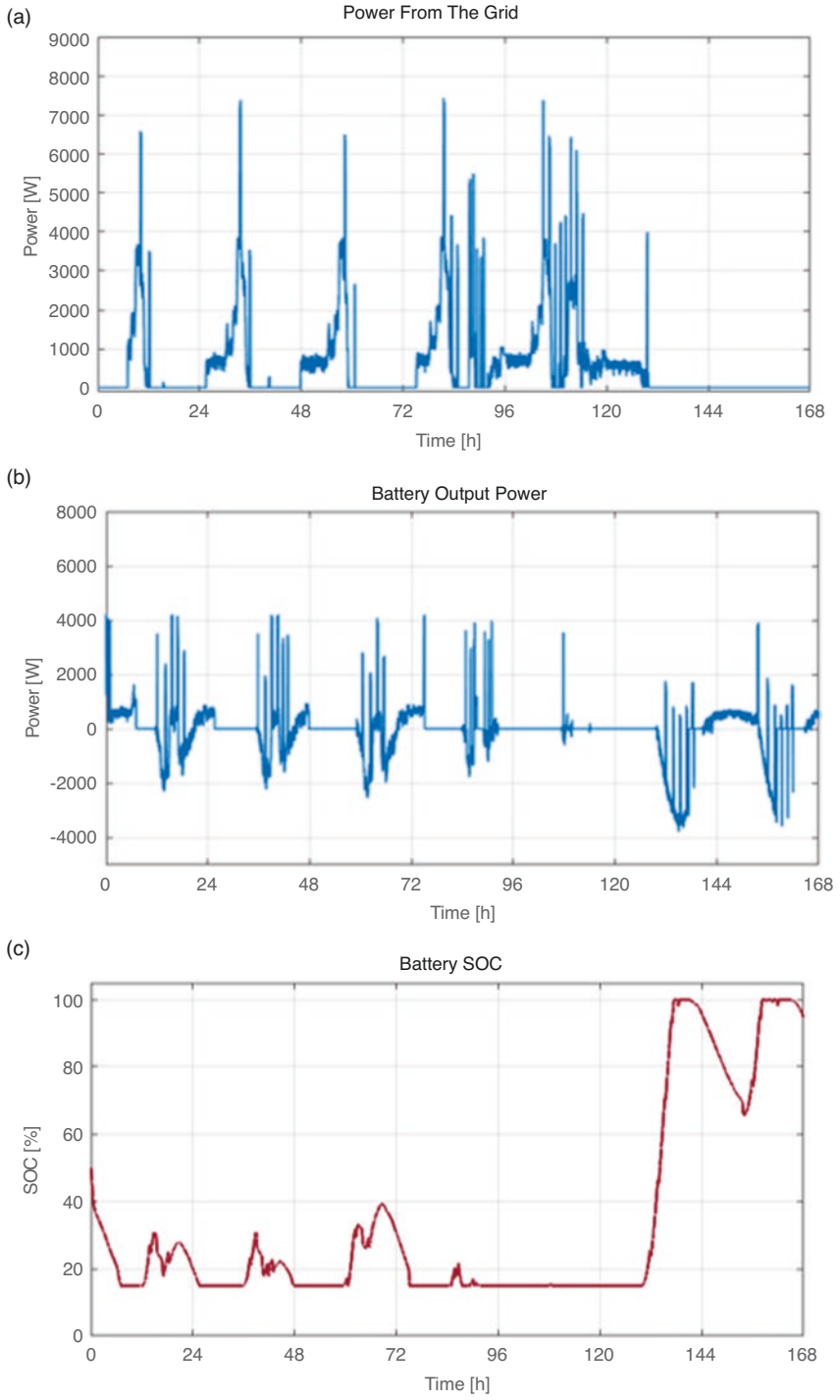

Fig. 10 Microgrid power outputs for the modified case in a week in July: (**a**) power extracted from the utility grid, (**b**) battery output power, (**c**) battery SOC

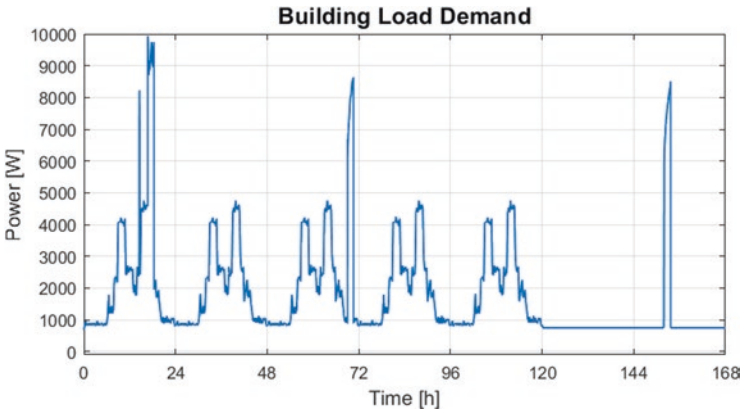

Fig. 11 Microgrid building load demand for the modified case in winter

power from the utility grid. When the SOC is smaller than 30%, the energy storage systems charge with power from the grid if the price is smaller than the median of the energy prices during the day. The battery charges from the grid with a constant power of 1500 W.

To avoid oscillations in the battery during this charging process, a minimum time of 5 h was set for the battery to stay without charging from the grid. It should be noted that these conditions only apply before the end of the work week.

Case Study – Summer

As can be seen from Fig. 13, in this case, only in the first hours of the day the conditions for the battery to charge from the grid are met. Afterward, the battery SOC rapidly increases to values above 90%, and in the few occasions where it goes below this value, the energy prices are greater than the quartile 25 of the prices during that day.

The total energy consumption from the grid had a significant increase relative to the case without EMS, from 1.35 kWh to 13.35 kWh. This increase is due to the interval, in the beginning of the week, when the battery is charging with energy from the grid. The energy bill also increases from 5.76€ to 6.81€.

Case Study – Winter

As can be seen from Fig. 14, a considerable reduction in the maximum of power extracted from the grid is observed. With control strategy 1, this value decreases to 3.62 kW, a difference of 4.2 kW. Because the battery SOC increases substantially due to the process of charging from the utility grid during the peaks in the demand

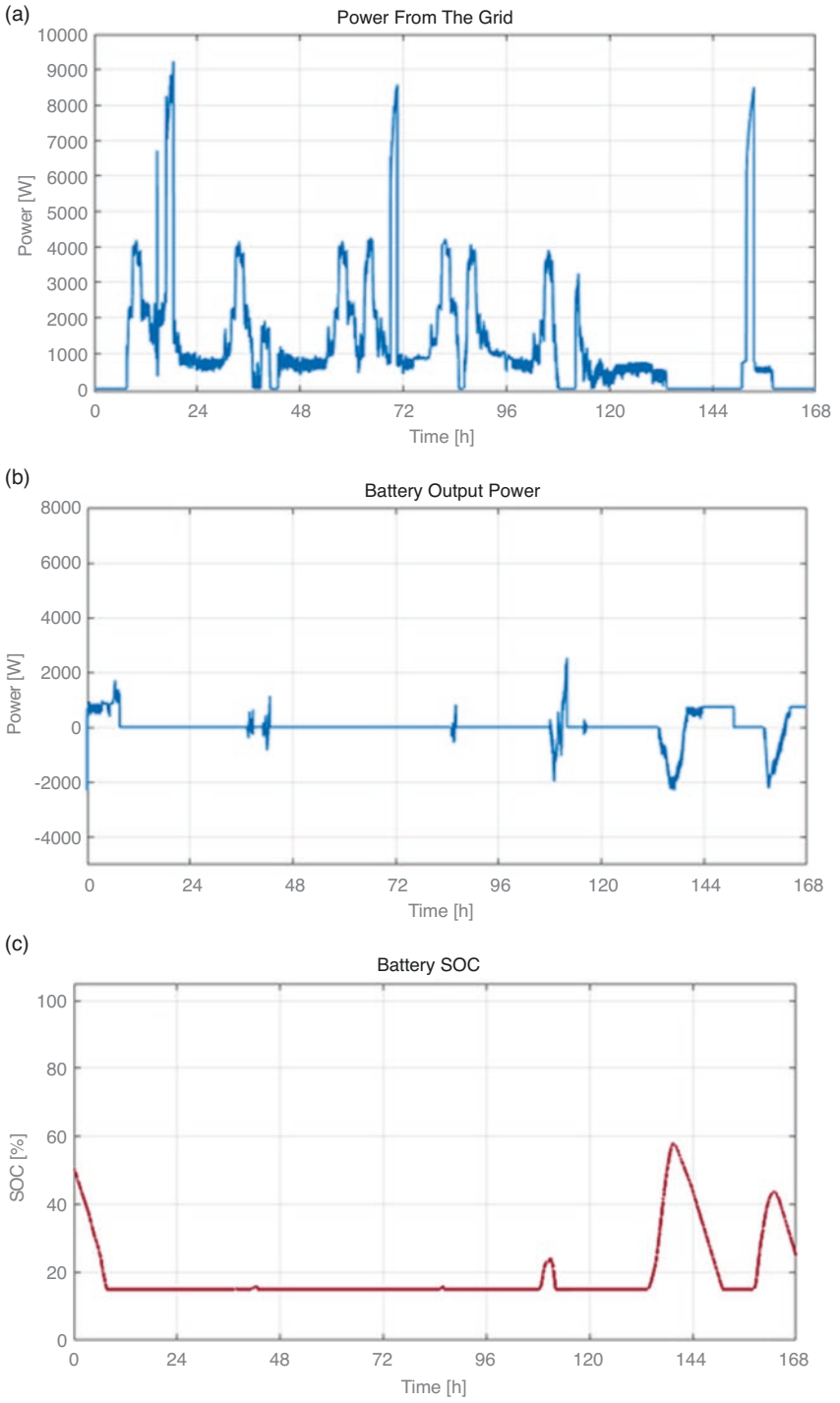

Fig. 12 Microgrid power outputs for the modified case in a week in January: (**a**) power extracted from the utility grid, (**b**) battery output power, (**c**) battery SOC

Fig. 13 Microgrid power outputs for the case in a week in January, control strategy 1: (**a**) power extracted from the utility grid, (**b**) battery output power, (**c**) battery SOC

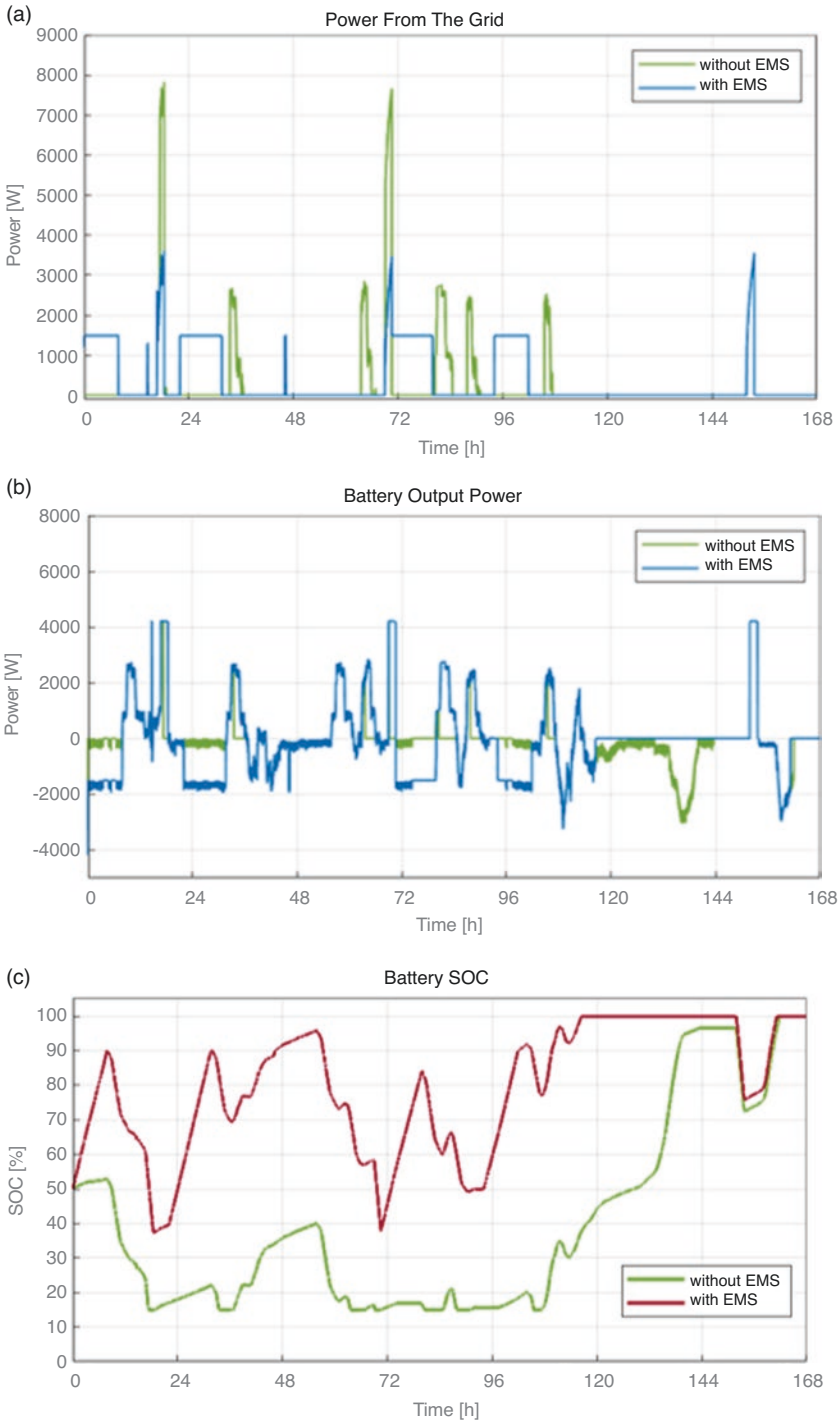

Fig. 14 Microgrid power outputs for the case in a week in January, control strategy 1: (**a**) power extracted from the utility grid, (**b**) battery output power, (**c**) battery SOC

(when the heat pump switches on), the battery has enough energy to fulfill the load until its maximum power output limit.

With this control strategy, the total energy consumption from the grid increases from 45.98 kWh to 65.66 kWh. Nonetheless, the energy bill sees a reduction from 13.60€ to 12.14€.

Modified Case Study – Summer

As can be seen from Fig. 15, the maximum power extracted from the grid suffers a slight reduction of 1 kW, and the battery, as expected, also attains higher levels than the case without EMS, due to the intervals when it was charging from the grid.

The total energy consumption from the grid only increases to 0.01 kWh in relation to the case without EMS. The energy bill reduced considerably, from 20.55€ to 17.01€. This decrease is mainly due to the allocation of power consumption from the utility grid when the energy prices were lower.

Modified Case Study – Winter

Figure 16 shows a very different behavior of battery SOC relative to the case without EMS. This control strategy presents six peaks during the working days, which occur when the battery is charging with power extracted from the utility grid. The total consumption of energy from the grid and the maximum of the power extracted from the grid had the same value as the case without EMS. The energy bill decreased from 38.19€ to 35.80€.

Control Strategy 2

This control strategy builds upon strategy 2. The on-off control described before was kept, and a new control block was added. Thus, when the result of the first part of the heat pump control is to switch on, the second block checks if the average temperature of the five condition spaces is within the comfort range (between 20 °C and 25 °C). If it is, the heat pump is turned off. If not, the SOC of the battery is evaluated. In case the SOC is lower than 50% and the energy price is greater than the daily median, the heat pump switches/stays off; otherwise it switches on. Because the effect of this control strategy in both cases for each season is similar, only the modified case study will be discussed in detail here (Fig. 17).

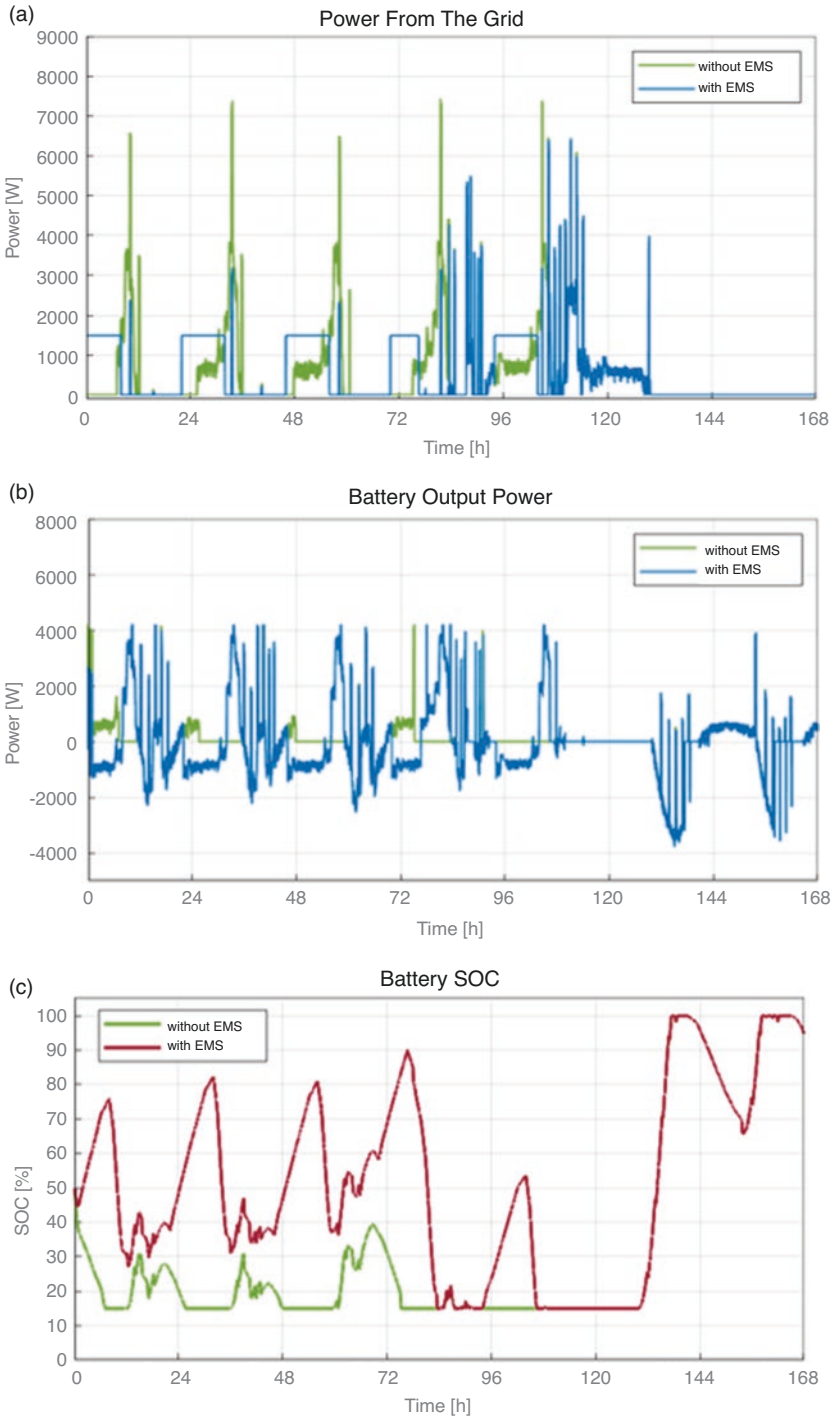

Fig. 15 Microgrid power outputs for the modified case in a week in July, control strategy 1: (**a**) power extracted from the utility grid, (**b**) battery output power, (**c**) battery SOC

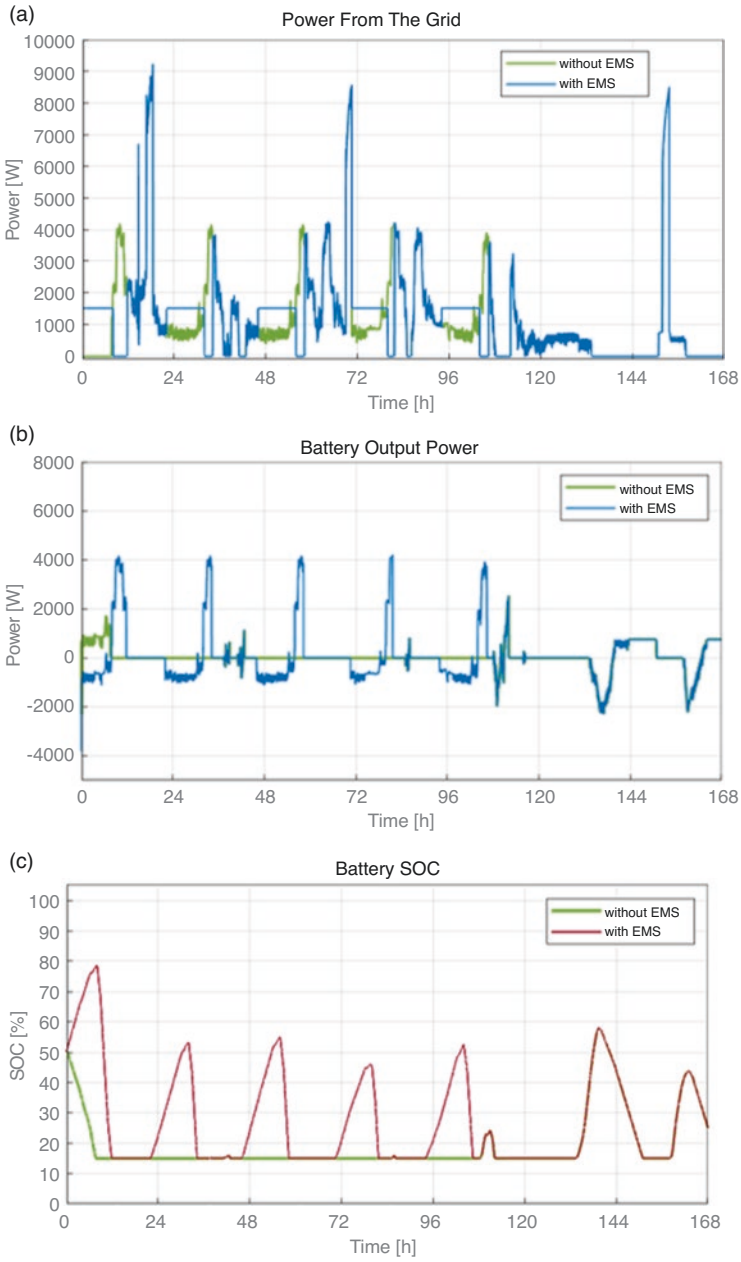

Fig. 16 Microgrid power outputs for the modified case in a week in January, control strategy 1: (**a**) power extracted from the utility grid, (**b**) battery output power, (**c**) battery SOC

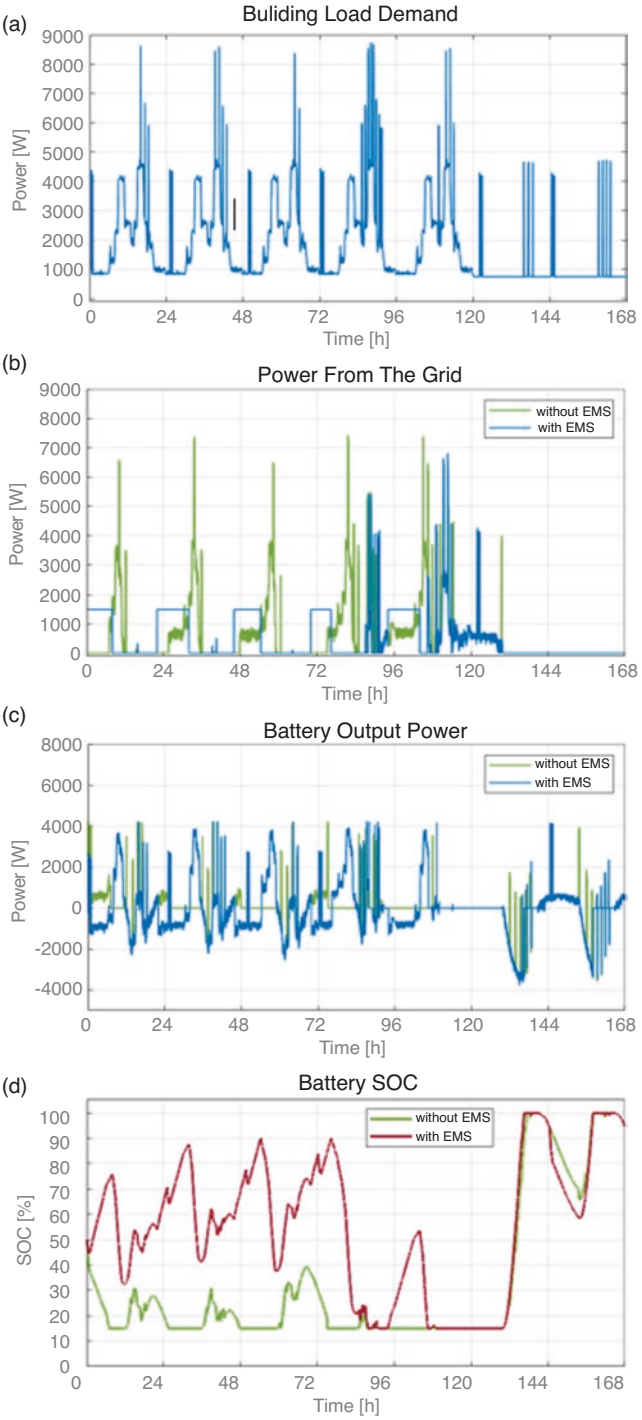

Fig. 17 Microgrid power output for the modified case in a week in July, control strategy 2: (**a**) building load demand, (**b**) power extracted from the utility grid, (**c**) battery output power, (**d**) battery SOC

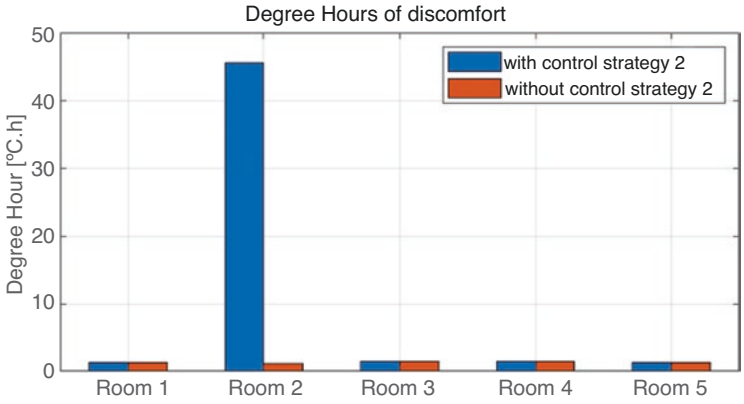

Fig. 18 Degree hours of discomfort for the modified case study for a week in July with control strategy 2

Modified Case Study – Summer

The heat pump switches on fewer times but with a slightly higher power than the case without EMS. The total energy consumed by the heat pump decreased by 28.5%, from 40.72 kWh to 29.12 kWh.

Both the maximum of the power and total energy consumption from the grid decreased to 6.8 kW and 89.73 kWh, respectively. The latter represents a reduction of 8.4% relative to the case without EMS.

The energy bill reduced by 24.4% in relation to the case without EMS, from 20.55€ to 15.53€.

Figure 18 demonstrates that except for room 2, the values of the degree.hours of discomfort are similar for both cases.

In room 2, this value increased from 1.216 °C.h to 45.61 °C.h, representing an average difference of 0.83 °C from the comfort temperature range.

This discomfort can be explained by the fact that as seen in [22], this space is the one with the worst cooling performance due to an excess of thermal loads in the room.

The new control block considers only the average temperature of all rooms. If the latter remains within the comfortable range, even if room 2 by itself is not within that range, the heat pump will stay off. This causes room 2 to reach even higher discomfort levels.

Modified Case Study – Winter

The heat pump switches on several times with control strategy 2. Nonetheless, the total energy consumption of the heat pump decreased from 34.92 kWh to 25.98 kWh (less than 25.6%).

Figure 19 presents the new load demand curve for the modified case study during a week in January and the power consumption from the grid, battery power output power, and battery.

SOC values with and without control strategy 2.

One can see that the maximum of the power consumption from the grid slightly decreased with this algorithm. The total consumption of energy from the utility grid is 190.9 kWh, and it represents a decrease of 5% relative to the case without EMS (199.8 kWh). The energy bill at the end of this week is 34.33€, a decrease of 10.1%.

The levels of thermal discomfort with and without this control strategy are similar and approximately zero.

Discussion

For the *case study* in summer, the lowest energy bill is attained for the case without EMS. This solution is also the one in which the building's energy consumption is lower, making it the preferable solution.

For the case study in winter, control strategy 1 results in a reduction of 11% in the energy bill in relation to the base case, but the energy consumption from the grid increases to 43%. With control strategy 2, the energy consumption from the grid is 26% higher than that for the base case. Still, it is lower than that for control strategy 1 and reduces the energy bill by 7%. Considering that the discomfort levels are zero for strategy 2, it seems to be the best option.

For the *modified case study*, in summer and winter, with control strategy 1, the energy consumption from the grid barely changes from the case without EMS, and the price reduces to 17% in summer and 6% in winter relative to the base case (Table 3).

For the winter case, the preferable control strategy is, again, the second one. It has the lowest energy consumption from the grid (decreases by 5%) and energy bill (decreases by 10%) and the same thermal comfort levels.

In the summer case, the second control strategy would also be the best one if only the decreases of 24% in the energy bill and 8% in the energy consumption from the grid were considered. However, the thermal discomfort levels in room 2 cannot be ignored, even though some things should be noted. First, this room serves as a meeting room that is only used during short periods of time and not in a daily basis. Second, the temperature is never more than one degree above the thermal comfort limit.

It is important to note that the relatively good thermal and lighting performance is largely due to the bioclimatic conception of the building – which is an essential first step to achieve the desired nZEB goals.

Finally, it is observed that the improvement obtained from applying these strategies is more significant for the modified case, where the loads are higher and the battery capacity is lower.

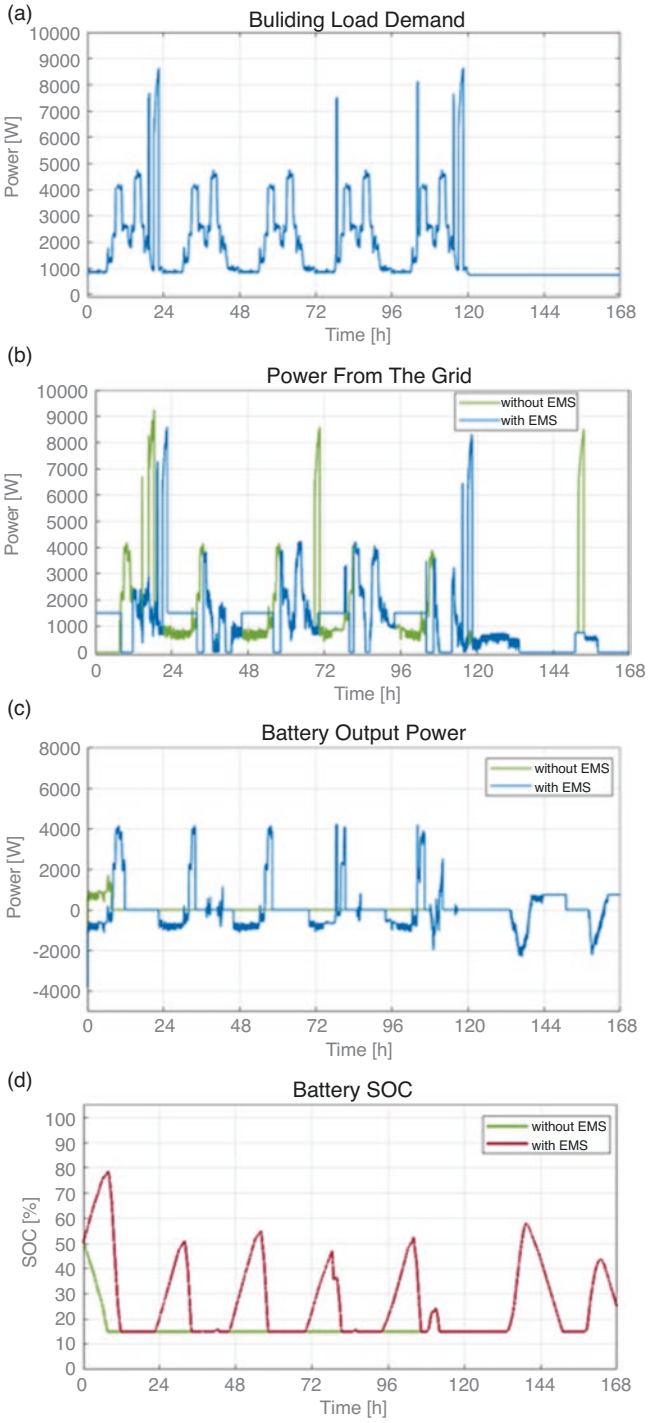

Fig. 19 Microgrid power outputs for the modified case in a week in January, control strategy 2: (**a**) building load demand, (**b**) power extracted from the utility grid, (**c**) battery output power, (**d**) battery SOC

Table 3 Comparison of the results with and without different control strategies for the case study and modified case study in both seasons

	Without EMS		ControlStrategy1		ControlStrategy2	
Case study	Summer	Winter	Summer	Winter	Summer	Winter
Price (€)	5.76	13.60	6.81	12.14	6.57	12.69
Energy from grid (kWh)	1.35	45.98	13.35	65.66	12.18	58.06
Pmax from grid (kW)	1.83	7.82	1.84	3.62	1.5	3.49
Heat pump energy (kWh)	40.72	34.92	40.72	34.92	29.15	26.75
Energy consumption (kWh)	136.3	130.5	136.3	130.5	124.7	122.3
Energy generation (kWh)	238.8	101.9	238.8	101.9	238.8	101.9
	Without EMS		ControlStrategy1		ControlStrategy2	
Modified case study	Summer	Winter	Summer	Winter	Summer	Winter
Price (€)	20.55	38.19	17.01	35.8	15.53	34.33
Energy from grid (kWh)	97.91	199.8	97.92	199.8	89.73	190.9
Pmax from grid (kW)	7.43	9.24	6.42	9.24	6.80	8.60
Heat pump energy (kWh)	40.72	34.92	40.72	34.92	29.12	25.98
Energy consumption (kWh)	312	306.2	312	306.2	300.4	297.3
Energy generation (kWh)	238.8	101.9	238.8	101.9	238.8	101.9

In future, it would be worthwhile to test these strategies on the real building and compare the resulting experimental data with that of the simulations. An enhancement of the proposed strategies should address the issue found in room 2, where the current approach fails to keep the temperature within comfortable levels. The analysis done in this study suggests that this could be achieved by controlling the heat pump with room temperatures, rather than their average, as input.

Appendix

Fig. 20
Fig. 21
Fig. 22
Fig. 23

Fig. 20 The LNEC. South façade (above), East façade (below)

Fig. 21 The atrium: bioclimatic design for daylight and natural ventilation

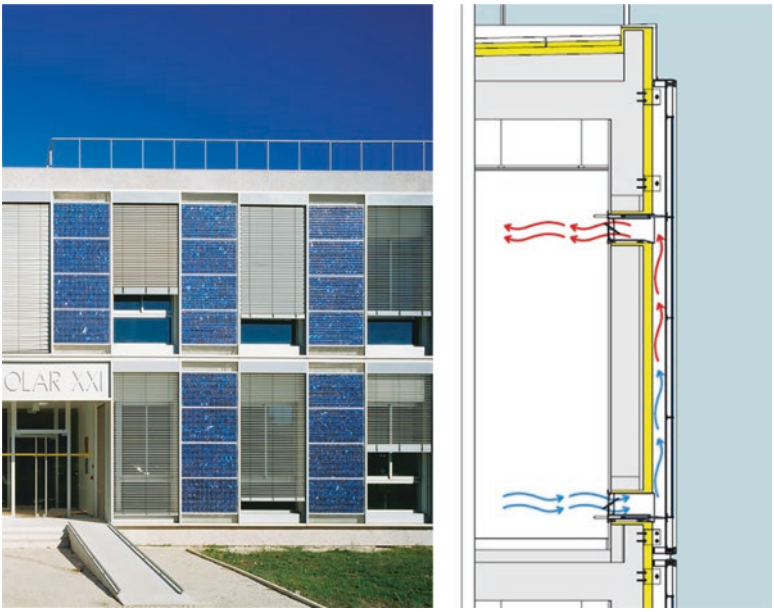

Fig. 22 Integration of PV in the South Façade, doubling as Trombe walls for winter heating

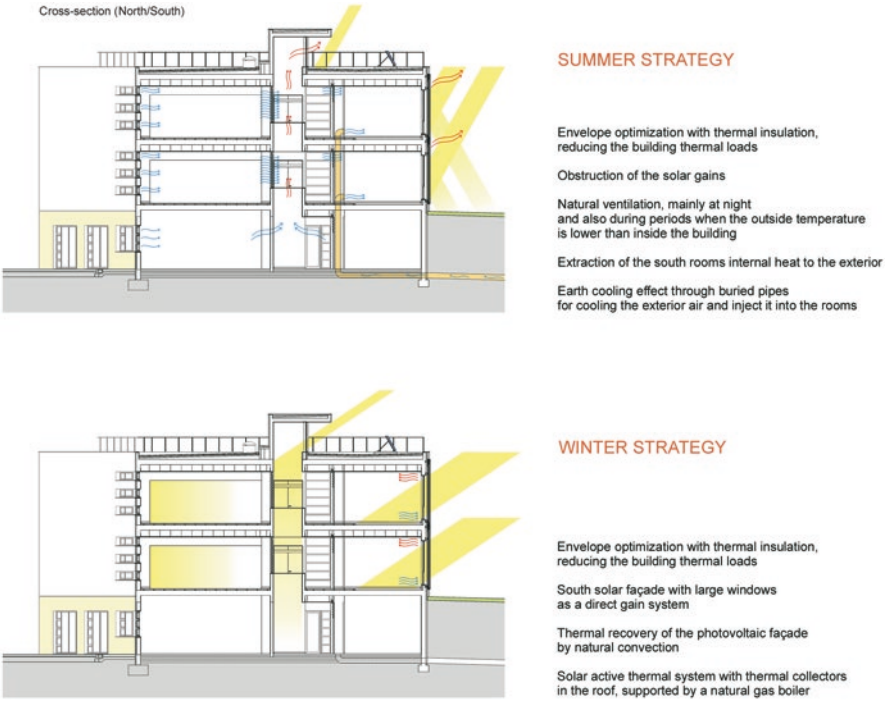

Fig. 23 LNEC: winter and summer bioclimatic design strategies

References

1. National energy and climate plans (NECPs) | Energy. https://ec.europa.eu/energy/topics/energy-strategy/national-energy-climate-plans_en. Accessed 27 Dec 2021.
2. Energy performance of buildings directive | Energy. https://ec.europa.eu/energy/topics/energy-efficiency/energy-efficient-buildings/energy-performance-buildings-directive_en. Accessed 27 Dec 2021.
3. National energy and climate plan 2021–2030 (NECP 2030), 2019, [online]. https://ec.europa.eu/energy/sites/default/files/documents/pt_final_necp_main_en.pdf. Accessed 27 Dec 2021.
4. Desempenho energético de edifícios. https://www.dgeg.gov.pt/pt/areas-setoriais/energia/energias-renovaveis-e-sustentabilidade/desempenho-energetico-de-edificios/. Accessed 7 May 2022.
5. Improvement | lneg Laboratório Nacional de Energia e Geologia. https://www.lneg.pt/en/project/improvement-2/. Accessed 3 Jan 2022.
6. Ton, D. T., & Smith, M. A. (2012). The U.S. department of energy's microgrid initiative. *The Electricity Journal, 25*(8), 84–94. https://doi.org/10.1016/j.tej.2012.09.013
7. Abdelgawad, H., & Sood, V. K. (2019). A comprehensive review on microgrid architectures for distributed generation. In *2019 IEEE electrical power and energy conference (EPEC)* (pp. 1–8). IEEE. https://doi.org/10.1109/EPEC47565.2019.9074800
8. Dorf, R. C. (2017). Energy management. In *Systems, controls, embedded systems, energy, and machines* (pp. 261–270). CRC Press.
9. Su, W., & Wang, J. (2012). Energy management systems in microgrid operations. *The Electricity Journal, 25*(8), 45–60. https://doi.org/10.1016/j.tej.2012.09.010

10. Khan, M. W., Wang, J., Ma, M., Xiong, L., Li, P., & Wu, F. (2019). Optimal energy management and control aspects of distributed microgrid using multi-agent systems. *Sustainable Cities and Society, 44*, 855–870. https://doi.org/10.1016/j.scs.2018.11.009
11. Fontenot, H., & Dong, B. (2019). Modeling and control of building-integrated microgrids for optimal energy management – A review. *Applied Energy, 254*, 113689. https://doi.org/10.1016/j.apenergy.2019.113689
12. Yamashita, D. Y., Vechiu, I., & Gaubert, J.-P. (2020). A review of hierarchical control for building microgrids. *Renewable and Sustainable Energy Reviews, 118*, 109523. https://doi.org/10.1016/j.rser.2019.109523
13. Grosan, C., & Abraham, A. (2011). Rule-based expert systems. *Intelligent Systems Reference Library, 17*, 149–185. https://doi.org/10.1007/978-3-642-21004-4_7
14. Elmouatamid, A., Ouladsine, R., Bakhouya, M., El Kamoun, N., Khaidar, M., & Zine-Dine, K. (2021). Review of control and energy management approaches in micro-grid systems. *Energies, 14*(1). https://doi.org/10.3390/en14010168
15. Naidu, D. S. (2003). Optimal control. In *Optimal control systems* (1st ed.). CRC Press.
16. Dou, C., Lv, M., Zhao, T., Ji, Y., & Li, H. (2015). Decentralised coordinated control of microgrid based on multi-agent system. *IET Generation, Transmission & Distribution, 9*(16), 2474–2484. https://doi.org/10.1049/iet-gtd.2015.0397
17. Garcia-Torres, F., Zafra-Cabeza, A., Silva, C., Grieu, S., Darure, T., & Estanqueiro, A. (2021). Model predictive control for microgrid functionalities: Review and future challenges. *Energies, 14*(5), 1296. https://doi.org/10.3390/en14051296
18. Parejo, A., Sanchez-Squella, A., Barraza, R., Yanine, F., Barrueto-Guzman, A., & Leon, C. (2019). Design and simulation of an energy homeostaticity system for electric and thermal power management in a building with smart microgrid. *Energies, 12*(9), 1806. https://doi.org/10.3390/en12091806
19. Chapaloglou, S., et al. (2021). Microgrid energy management strategies assessment through coupled thermal-electric considerations. *Energy Conversion and Management, 228*, 113711. https://doi.org/10.1016/j.enconman.2020.113711
20. Biyik, E., & Kahraman, A. (2019). A predictive control strategy for optimal management of peak load, thermal comfort, energy storage and renewables in multi-zone buildings. *Journal of Building Engineering, 25*, 100826. https://doi.org/10.1016/j.jobe.2019.100826
21. Pombeiro, H., Machado, M. J., & Silva, C. (2017). Dynamic programming and genetic algorithms to control an HVAC system: Maximizing thermal comfort and minimizing cost with PV production and storage. *Sustainable Cities and Society, 34*, 228–238. https://doi.org/10.1016/j.scs.2017.05.021
22. Guedes, M. C., & Cantuaria, G. (Eds.). (2019). *Bioclimatic architecture in warm climates: A guide for best practices in Africa*. Springer. ISBN 978-3-030-12035-1.
23. da Silva, M. A. G. (2021). *Renewable based thermal systems for microgrids*. Instituto Superior Técnico, Universidade de Lisboa.
24. Coelho, M. Q. S. (2021). *Renewable power systems for microgrids in public buildings*. Instituto Superior Técnico, Universidade de Lisboa.
25. Tabela de Preços 2022 – Mercado Regulado. https://www.celoureiro.com/pdf/precos/2022/Tabela de Precos 2022 – Tarifas Transitoria – Mercado Regulado.pdf. Accessed 12 May 2022.
26. ERSE – Tarifas e preços – eletricidade. https://www.erse.pt/atividade/regulacao/tarifas-e-precos-eletricidade/#periodos-horarios. Accessed 12 May 2022.